RSC Advances

ROYAL SOCIETY OF CHEMISTRY

www.rsc.org/advances

Journal Name

RSCPublishing

ARTICLE

Graphene quantum dots cutting from graphene flakes: high electrocatalytic activity for oxygen reduction and low cytotoxicity

Cite this: DOI: 10.1039/x0xx00000x

Received 00th January 2012,
Accepted 00th January 2012

DOI: 10.1039/x0xx00000x

www.rsc.org/

Rui Yan [a,b], Hao Wu [c], Qing Zheng [c], Junying Wang [a], Jianlin Huang [a], Kejian Ding*[c], Quangui Guo[a], Junzhong Wang*[a]

3-8 nm size of high quality of graphene quantum dots with zigzag edges and multi-heteroatom doping were synthesized through a green process of electrochemically cutting pristine few-layer graphene flakes. The graphene quantum dots exhibit the structure features of monodisperse and shaped nanocrystals co-doped by O, N and F elements or chemical groups mainly at zigzag edges. The cutting and in-situ doping of the graphene flakes into dots were realized in the potential/current exchangeable electrochemical etching process without any thermal treatment. It was found that the graphene dots showed high electrocatalytic activity for oxygen reduction reaction including 70 times enhancement in voltametric current in oxygen saturated KOH compared to that in nitrogen. In addition, low in-vitro cytotoxicity and fluorescent labeling to Vero cells and NRK cells of the graphene dots were presented. The Gdots synthesized may potentially be applied in the fields of electrocatalysis and biomedicine.

1. Introduction

It is important to obtain electrocatalysts for power supply without risks to human health or the environment. The oxygen reduction reaction (ORR) has attracted intense attention in the past decades owing to its importance to and continued challenges for several energy applications including fuel cells[1] and metal-air batteries[2]. Platinum-based materials are known to be the most active catalysts for ORR in both alkaline and acidic conditions, but their commercialization are impeded by high cost and inferior durability.[3] Therefore, the search for non-precious-metal as well as metal-free catalysts for ORR becomes one of the most competitive fields in chemistry and electrochemictry.[4,5] In recent years, heteroatom-doped carbon-based nanomaterials as a new type of metal-free ORR electrocatalysts have received a growing interest.[5] When a carbon framework is bonded with a heteroatom, a defect is induced in the nearby sites owing to different bond length and atomic size, which thus alters the electronic properties of carbon framework including uneven but table charge distribution.[6] The unique structure may contribute to superior ORR electrocatalytic performance.[7] Among the doped carbon materials, N-doping has been a popular choice.[8-10] N-doped carbon nanotubes,[11,12] ordered mesoporous graphitic arrays, [13,14] and graphene sheets[15,16] have been investigated to exhibit potential high electrocatalytic activities for ORR. However, the catalytic activities are highly dependent on the synthesis processes of these materials, often involving thermal treatment at high temperature. Moreover, it is not yet well-understood whether the catalytic activity for ORR of a carbon material doped by a usually low content of heteroatoms is caused by its doping electronic properties or metal residue from its preparation process.[11,17]

Graphene, a two-dimensional sp2-carbon bonding matter has attracted extremely intense attention for its outstanding conductive, electronic, optical and mechanical properties.[18] On the other hand, graphene is a zero-bandgap material, which impedes its application in the fields of bandgap-dependent electronic devices and fluorescence-dependent optoelectronics and biology.[19] In addition, unlike graphene oxide,[15,16,20] pristine graphene is hard to heteroatom-doping. So the properties of combining graphene and the heteroatom-doping are far from real investigation. Consequently, Graphene dots (Gdots) that are single- or few-layer graphene with a tiny size of only several nanometers, have emerged because of a great potential of quantum confinement and rich edge effects as well as various available chemical doping.[21]

Various synthesis methods have been tried to make Gdots. Till now, they can be roughly divided into two categories: bottom-up and top-down approaches.[21-30] Bottom-up growth mainly includes other carbon source conversion, such as organic chemical synthesis,[22] substrate-induced C_{60} transformation,[23] and hydrothermal carbonization.[24] The top-down routes for Gdots synthesis involve chemical oxidation,[25] hydrothermal treatment [26,27] or a microwave assisted reaction (reduced) graphene oxide [28] and electrochemical oxidation of graphite [29,30] and reduced graphene oxide.[10] However, most cases often use hazardous and corrosive reagents and are also hard to be rationally controlled. It is well accepted that soft chemical approaches have succeeded in synthesizing traditional

semiconductor quantum dots (nanocrystals) or metal nanoparticles through rational control of size, shape, composition and structure.[28] However, in contrast, it is quite challenging for precise control of size, shape, composition, and structure of graphitic nanoparticles, thus it is also difficult for Gdots to find the relationship between structure and properties or catalytic mechanism. In addition, few work concerns the cytotoxicity of the doping Gdots.[21,30]

In a previous work, the graphite as starting material was electrochemically oxidized to broad-size graphene products including graphene nanoparticles.[31] In another previous work, pristine few-layer graphene flakes from graphite direct exfoliation at high yield have been synthesized.[32] Thus, it is interestingly available to investigate whether and how to tailor graphene flakes into what kind of graphene dots. Herein, we present a green method of cutting pristine graphene flakes into high quality of Gdots through electrochemical charging reversely in ion liquid/water solution. This kind of synthesis method of Gdots didn't involve any thermal treatment and any toxic chemicals. Various characterization techniques including electron microscopes were comparatively analysed graphene flakes and dots converted. The Gdots exhibit the features of zigzag edges and several kinds of heteroatoms including N-doping and O-doping at the same time. Interestingly, the Gdots as a metal-free electrocatalyst showed good oxygen reduction catalysis properties. The 70 times enhancement of the current density of oxygen saturated KOH solution compared to nitrogen saturated condition was achieved. In addition, in-vitro cytotoxicity to and fluorescent imaging for two kinds of animal cells was investigated, and a bit of cytotoxicity to Vero cells and NRK cells was found.

2. Experimental Section

2.1 Chemicals and Materials.

1-butyl-3-methylimidazolium tetrafluoroborate was purchased from Linzhou Keneng Material Technology CO.,LTD. The following chemicals were obtained from Sinopharm Chemical Reagent and used without further purification: lithium perchlorate ($LiClO_4$ powder, 98%, weight percentage), propylene carbonate (PC, anhydrous, 99.7%), lithium chloride (LiCl, 99%), ammonia (28%), N,N-dimethylformamide (DMF), hydrochloric acid (HCl, ~37%).

2.2 Synthesis of graphene quantum dots (Gdots).

Graphene flakes were prepared from natural graphite powder by electrochemical method reported in previous paper.[32] The electrochemical preparation of Gdots was performed in an electrolyte solution of water and ionic liquid (IL) of 1-butyl-3-methylimidazolium tetrafluoroborate ([Bmim][BF_4]). Briefly, two pieces of porous plastic tubes loaded graphene flakes powder (1 g) were used as both negative and positive electrodes. The electrodes were immersed into the solution of IL/water (3/1, v/v) with a distance of 1.0 cm. Static potential of 10 V was applied to the two electrodes, with the exchange of current direction in every eight hours. After three days of charging, the electrolyte solution was found to change from colorless to yellow and finally to a dark brown color. Then the electrolyte solution was centrifuged to remove the black precipitate, and the above solution was dialyzed in 100Da dialysis bag against deionized water for a number of times and for several days. A light yellow powder of GQDs was obtained through centrifugation and freeze-drying.

2.3 Characterizations.

Scanning electron microscopy (SEM) images were obtained on a JSM-7001F FESEM (Field emission scanning electron microscopy). Transmission electron microscopy (TEM) images were obtained with a JEM- 2100F microscope at an acceleration voltage of 200 kV. The samples were supported on ultrathin carbon film-supported Cu TEM grids. X-ray powder diffraction (XRD) was recorded at a scan rate of 0.02°/s using the Cu Kα (1.540600 Å) line. XPS measurements were performed using a Thermo ESCALAB 250 spectrometer, employing an Al-KR X-ray source with a 500 μm electron beam spot. Raman data were measured in a Jobin-Yvon HR-800 Raman system with the 488 nm line of an Ar laser as excitation source. The Fourier transform infrared spectroscopy (FTIR) spectra were recorded on a VERTEX70 (Bruker) spectrometer with the KBr pellet technique ranging from 500 to 4000 cm^{-1}. The UV-vis absorption measurement was performed on a Hitachi UV 2800 spectrophotometer. The fluorescence spectra of the GQDs were measured with a fluorescence spectrometer F-7000 (Hitachi, Japan). Thermal analysis (TG/DTA) was carried out using a thermal analyzer (Netzsch STA409PC) at a heating rate of 10 °C/min from 20 to 1000 °C in Ar. Electrochemical characterization was performed in Autolab instrument of PGSTAT204.

2.4 Electrochemical testing

A glassy carbon (GC) electrode was carefully polished with gamma alumina powder. Then the electrode was rinsed and fully sonicated with double distilled water to remove alumina residues. Finally, it was dried in vacuum. [33,34] In a mixture of 5% Nafion (40 μL) and ethanol (4 mL), the catalysts (4 mg) were dissolved by sonication. Then, the solution (20 μL) was drop-casted on the GC electrode surface (diameter 5 mm) and air dried. A platinum wire was used as the counter electrode and saturated calomel electrode (SCE) as the reference electrode. All the experiments were conducted at room temperature, in an O_2 or N_2-saturated 0.1 M KOH aqueous solutions. CV measurement and rotating disk electrode (RDE) voltammetry were all performed using a Autolab electrochemical analyzer and a MSR electrode rotator (PINE, USA) at different rotation rates. The scan rate is 50 mV/s for the CV measurements, and the scan rate is 10 mV/s at various rotating speeds for the LSV measurements.

2.5 Oxygen reduction reaction (ORR) activity calculation method.[13-15,35]

The ORR studies were conducted in an O_2-saturated KOH aqueous solution (0.1 mol/L) using a rotating disk electrode system (PINE). Prior to ORR measurements, the solution was bubbled with O_2 for 30 min. The transferred electron numbers per oxygen molecule involved in the ORR were determined using the Koutechy-Levich equation:

$$\frac{1}{J} = \frac{1}{J_k} + \frac{1}{B\omega^{1/2}}$$

where J is the measured current density, J_k are the kinetic- and diffusion-limiting current densities, B is the Levich constant, and ω is the electrode rotating rate. The transferred electron numbers per oxygen molecule can be calculated from the Levich constant as follows:

$$B = 0.62nFD^{2/3}\nu^{-1/6}C_0$$

where n is the transferred electron numbers per oxygen molecule, F is the Faraday constant (F = 96485 C/mol), D is the diffusion coefficient of O_2 in 0.1 M KOH (i.e., 1.9×10^{-5}

cm^2/s), v is the kinetic viscosity (0.01 cm^2/s), and C_0 is the bulk. concentration of oxygen (i.e., 1.2×10^{-3} mol/L).

2.6 In vitro cytotoxicity test of Gdots

The MTT (3-[4,5-dimethylthiazol-2-yl]-2,5 diphenyl tetrazolium bromide) assay was used to measure the Gdots' cytotoxicity. Typically, Vero cells were inoculated in 96-well microplate at a density of 2×10^3 per well and cultured in Dulbecco's Modified Eagle Medium (DMEM, Gibco, USA) under the conditions of 5% CO_2 and 96% relative humidity atmosphere and at 37℃. After the incubation for overnight, the GQDs solution was added into the culture media at a final concentration of 5, 10, 25, and 50 μg/ml. In every 24 hours, MTT assay was conducted as MTT protocol. The prepared MTT solution was added and incubated for another 4 h. Finally, the MTT containing media was removed and the insoluble purple formazan crystals produced by live cells were dissolved in 100 μL of dimethyl sulfoxide (DMSO). The absorbance was monitored at 570 nm by a microplate reader.

3. Results and discussion

Using few-layer graphene flakes as a starting material (Fig.1a,b), graphene quantum dots (G dots) were obtained through electrochemical charging/discharging at high voltage of 10V. The electrolyte is the solution of water and 1-butyl-3-methylimidazolium tetrafluoroborate [Bmim][BF_4] with the volume ratio of 1/3. The yellow Gdots in clear ion liquid solution could be precipitated out during the dialyzation in deionized water owing to the de-absorption of ion liquid onto Gdots. TEM imaging was applied to carefully analyse the colloidal particles. Fig.1c presented monodisperse particles with narrow size distribution of 3-8 nm and tiny sheet-shaped morphology. Those particles display single-crystalline shaped nanocrystals with a lattice spacing of 0.240-0.279 nm that is comparable to the (100) facet of graphite (Fig.1d). Notably, honeycomb lattices with zigzag edges of a 7 nm graphene dot were clearly observed by high resolution TEM, as shown in Fig.1e and illustrated in Fig.1f. The inset FFT of crystal lattice of the dot showed that the average distance is 0.265 nm. The TEM data proved that Gdots are highly crystalline graphene nanoparticles with zigzag edges.

The XRD pattern of graphene flakes appears a sharp and strong (002) peak at 2θ = 26.5º, but this peak in the Gdots sample becomes very weak, which indicates that Gdots are thinner than G flakes owing to the further exfoliation of few-layer graphene. The broad peak centered at around 21.9 degrees (d value ~0.405 nm) may result from the π-π stacking of Gdots. It was suspected that the weak peak at around 2θ= 28.3º (d = 0.316 nm) was from few-layer of graphene dots. No peak was observed in the region of 2θ = 5 - 20º, which evidently showed that the Gdots are distinct from graphene oxide. Thermal Gravimetry Analysis (TGA) of Gdots compared to the precursor ion liquid was presented in Fig. 2b. The continuous weight loss at the temperature of 200-600ºC in Gdots curve is quite different from the dramatic drop of 350-500ºC in ion liquid [Bmim][BF_4] curve, which suggested that the weight loss of Gdots sample probably resulted from chemical groups covalent linked to the edges of the Gdots rather than the evaporation or decomposition of the precursors absorbed onto Gdots. Fourier transform infrared spectroscopy (FTIR) spectra for the dry Gdots products compared to the precursors of the graphene flakes and ion liquid [Bmim][BF4] samples are showed in Fig.2c. The spectrum of the product Gdots is different from each of the precursor graphene flakes and ion liquid. The comparison of the ion liquid precursor with the Gdots product clearly presented that most of rich chemical groups in ion liquid disappeared in Gdots. For example, in ion liquid, the peaks at 3120 cm^{-1} and 3158 cm^{-1} as well as 1167 cm^{-1} are assigned to CH_3(N) stretching and CH_2(N) stretching and in-plane asymmetric stretching of imidazolium ring.[36-37] Those peaks disappeared completely in Gdots sample, which indicated that ion liquid was completely removed from Gdots and little imidazolium ring existed onto Gdots.[36] The strong broad peak at around 3425 and 1645 cm^{-1} are associated with the vibrations of O–H and C=O bonds, respectively, and a peak at 1078 cm^{-1} is related to C–O alkoxy groups onto Gdots (Fig. 2b).[37] Those data reflected that Gdots had many oxygenated functional groups on their surfaces, making them soluble in water. Raman analysis of graphene flakes and Gdots was shown in Fig.2d. The weak D and strong G band indicated of little-defective graphene flakes.[32] Much higher ratio of the intensity of D band over G band of Gdots than that of graphene flakes suggested that much more defects in Gdots because of much more edges of Gdots over flakes. Please note that the Raman signal was interfered by the fluorescence of the Gdots excited at 488 nm laser.

Journal Name

RSCPublishing

ARTICLE

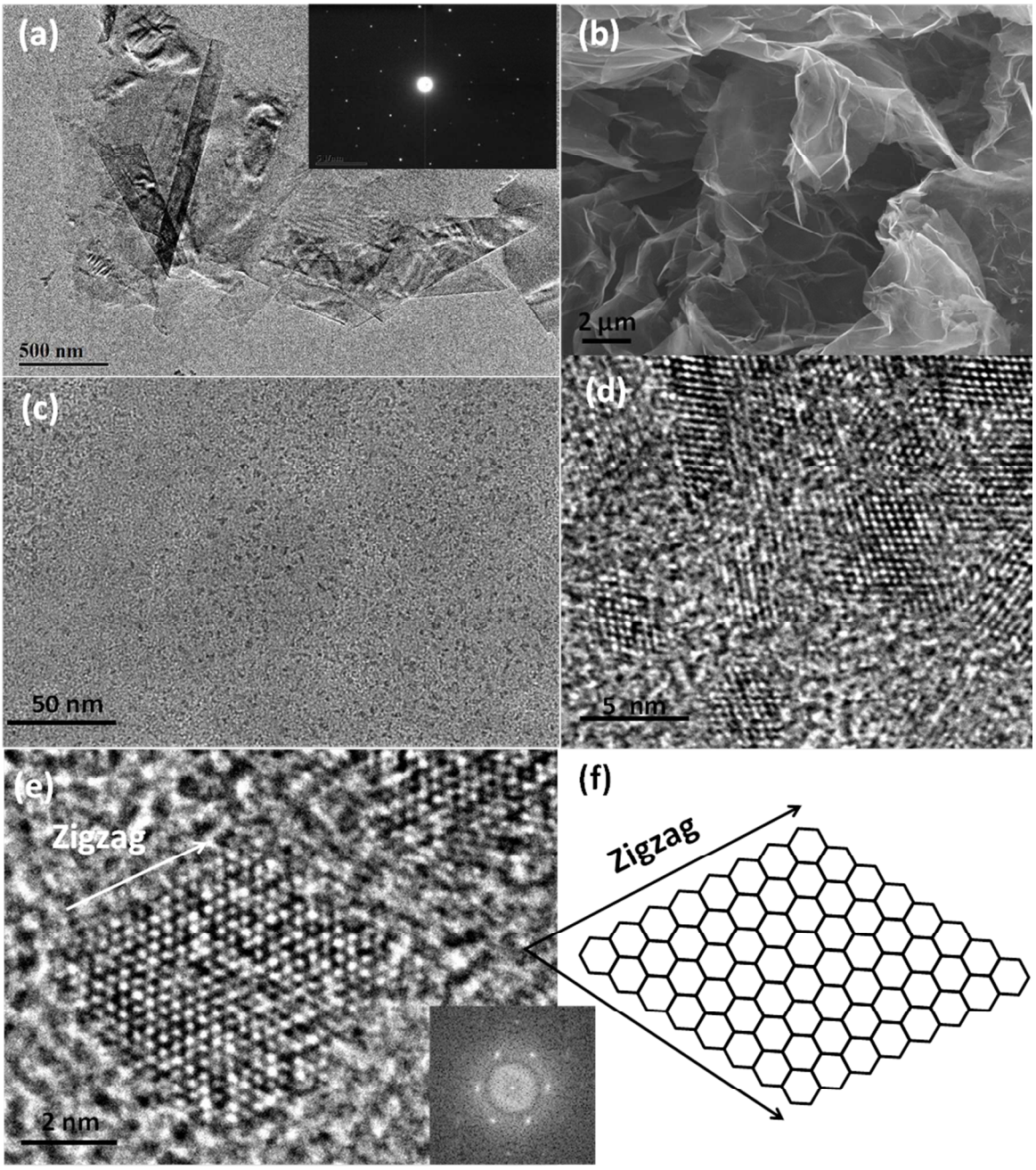

Fig. 1 Electron microscopy images of high quality of graphene quantum dots (Gdots) synthesized using pristine few-layer graphene flakes as a precursor. (a) TEM image of graphene flakes (inset the electron diffraction pattern) and (b) SEM image of graphene flakes. (c-e) TEM images Gdots. (c) Large area of Gdots with a colloidal dispersion, (d) 4-8 nm of Gdots with crystal lattices slightly deformed, (e) clear high resolution of TEM image of a graphene particle of 7 nm displays the zigzag edges (inset the FFT of the image), (f) schematic illustrating the graphene dot (e) with zigzag edges.

Journal Name

RSCPublishing

ARTICLE

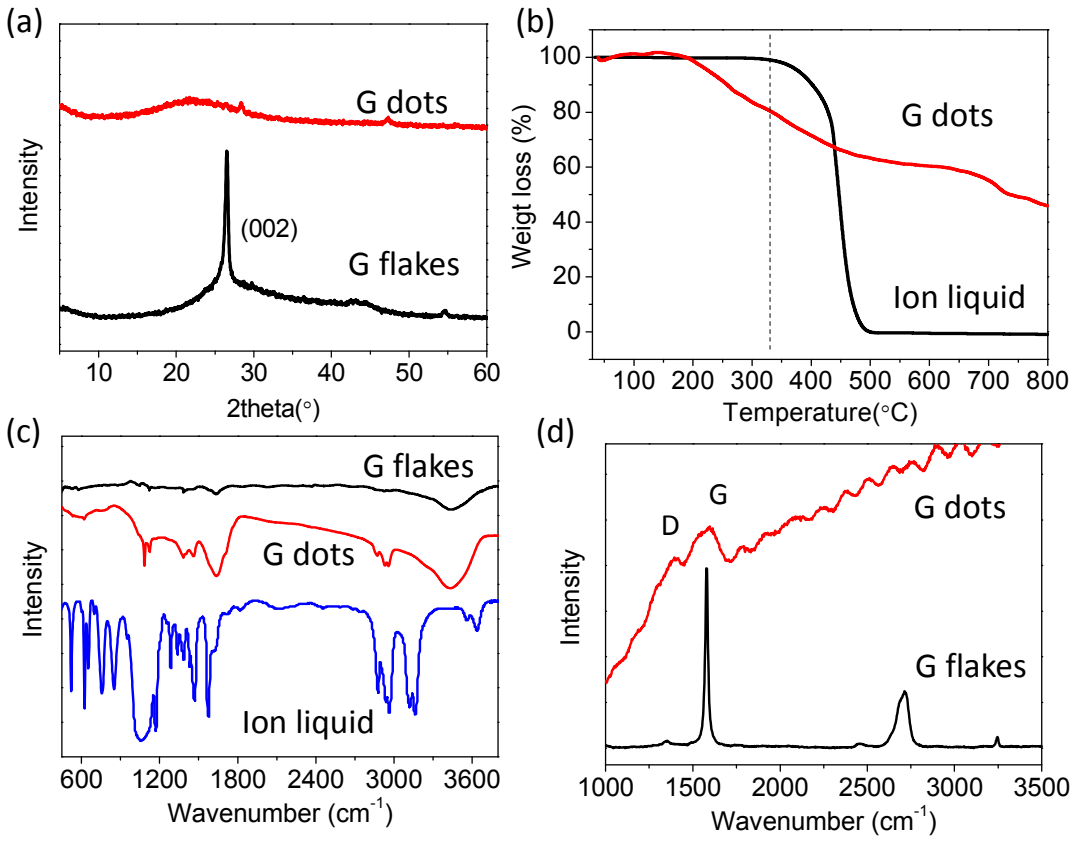

Fig. 2 Characterizations of graphene quantum dots (Gdots) compared to the precursor flakes and ion liquid. (a) XRD patterns of the powders, (b) TGA spectra. (c) FTIR spectra of powders, (d) Raman spectra excited at 488nm. The fluorescence of the Gdots caused by laser irradiation interfered Raman signal measurement.

The chemical doping information was analysed by X-ray photoelectron spectroscopy (XPS). Wide spectra in Fig.3a showed that multi-elements including C, O, N and F were found in Gdots while little N and F elements were detected in G flake precursor. It was calculated that the content of each element in Gdots is C 61.7%, O 26.3%, N 10.3% and F 1.7%, respectively. In contrast, G flakes has C 96.3% and O 3.7%. It was noted that little B element was detected, which suggested that F was not from the anion of BF_4^- of ion liquid. The high contents of the heteroatoms observed by XPS indicated of rich C-X (X=O, N, F) existing in the Gdots, which are in agreement with above TGA and FTIR data. Fine XPS measurements were used to further analyze these elements, as shown in Fig.3b-f. By curve-fitting analysis, the C1s spectrum results from five parts of C-C (285.0 eV), C-O (286.1 eV) (such as C-OH), C-N (287.2 eV), O-C=O/C-F (288.5 eV).[23-28,38] It is important to identify the chemical doping as either absorption doping or/and covalent bonding doping. The best fitting of N 1s spectrum indicates that Gdots have two types of N atoms.[7-10,15,16] The peak at 400.2 eV can be assigned to the N1s of pyrrolic N (the imidazolium group) absorbed or located at the graphitic edge. Quaternary N (~401.2 eV) atoms may be thought to be incorporated into the graphene layer and substitute carbon atoms within the graphene plane.[16,39,40] Based on all above spectral results, it is believable that the chemical doping of Gdots is a multi-element co-doping of O and N as well as F elements and the doping of chemical groups is not just from absorption-induced doping but includes heavy heteroatom-bonded doping. In addition, most of doping possibly was located at the edges of Gdots.

Journal Name RSCPublishing

ARTICLE

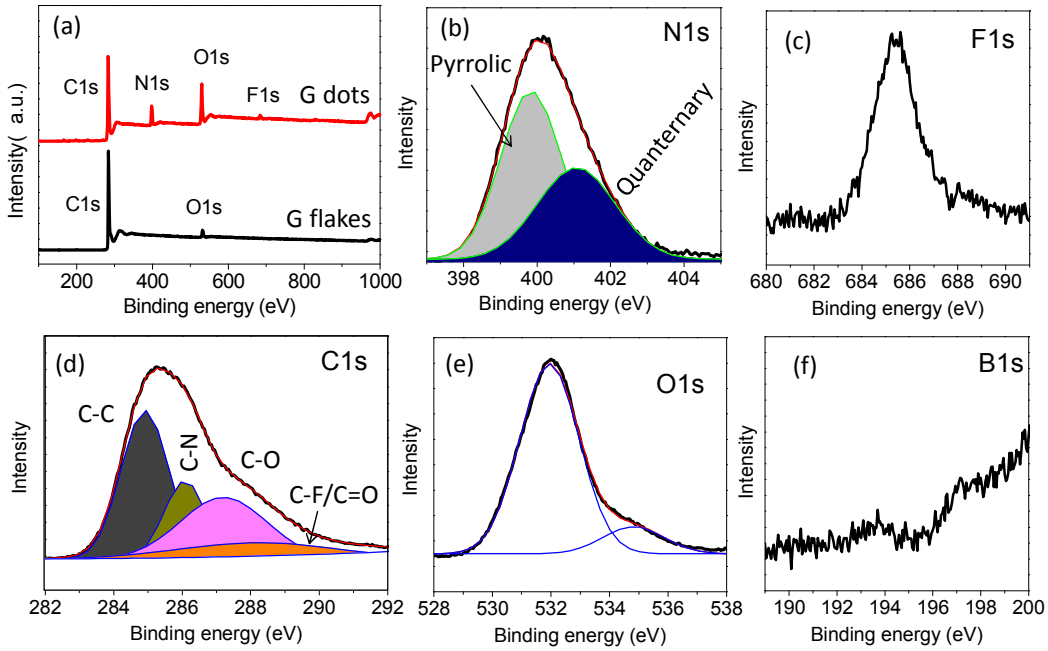

Fig. 3 X-ray photoelectron spectroscopy (XPS) spectra of Gdots. (a) Wide spectra of Gdots compared to graphene flakes. (b) N1s spectrum. Best fitting by pyrrolic and quanternary N atoms. (c) F1s spectrum. (d) C1s spectrum through best fitting by the C-C, C-N, C-O-H, C-F and O=C-OH groups. (e) O1s spectrum, (f) B1s spectrum.

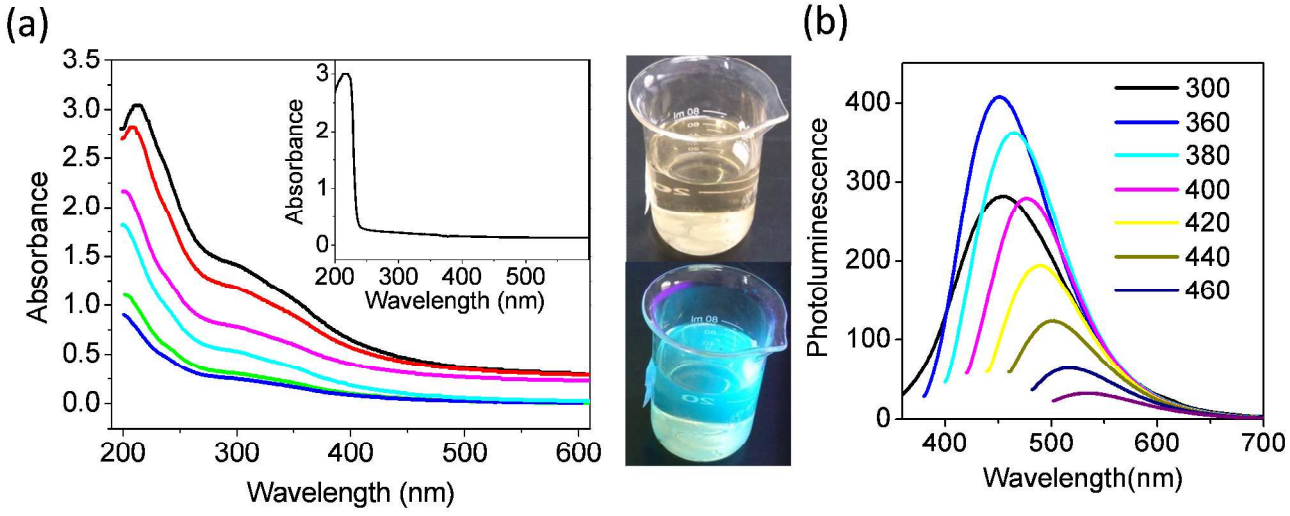

Fig. 4 Optical properties of Gdots. (a) concentration-dependent UV-Visible absorption spectra of Gdots in water, inset the absorption spectrum of graphene flakes, (b) photoluminescence spectra with various excitation wavelength. Inset optical and fluorescent (irradiated by 365 nm UV light) images of Gdots measured.

The optical properties of Gdots in water solution were shown in Fig.4. Compared to graphene flakes, the G dots show strong quantum absorption peaks at around 360 nm and 300 nm, corresponding to excitation wavelength (not presented). Photoluminescence (PL) measurement appeared excitation wavelength-dependent emission, which indicated of the non-uniformity fluorescence resulted from non-uniform size of Gdots, similar to many work reported.[25-28] The inset optical and bright fluorescent photographs under the UV lamp are also presented (the chemical of ion liquid has no fluorescence). The quantum yield of fluorescence is close to 15%, which may be related to the concentration-dependent absorption of graphene in high wavelength of > 500 nm. The Gdots powder after drying loss fluorescence but recovered after sonicating and hydrothermal treatment in water, which suggested that the water passivation was important for the fluorescence.

It should be pointed out that our starting material of graphene flakes shows the features of little defects and high crystallinity. As expected, higher quality of Gdots than the products from graphene oxide were obtained through electrochemical redox process following dialyzation in deionized water.[10,26,28] The electrochemical oxidative etching mechanism of graphite was discussed in a previous work.[31] Here there is something different. The electrolysis of water at high potential of 10V leads to H_2 and O_2 evolution, and the current direction exchange involved complex redox reactions of ions at each graphene electrode. For example, imidazolium cation could be bonded onto graphene negative electrode and further oxidized for re-organization at positive electrode after in turn exchange of potential and current. It was observed that pH value increased from 7.0 to 10.0 after charging 3 days, which should be resulted from faster evolution of H_2 than O_2 in the electrolyte.[31,41] As schematically illustrated in Fig.5a, graphene flake was electrochemically oxidized and reduced in turn with multi-elemental doping. The basic condition may contribute to the corrosive etching of graphene flakes. Since the anion OH^- is less stable than BF_4^-, OH^- tends to loss an electron and change to radical of HO• that can react with graphene carbon-carbon bonding. Zigzag edges of graphene were usually thought to be stable than armchair one,[42] so the zigzag edges of graphene were dominantly produced.[25] It was observed that nanosheets and line consists of Gdots (Fig.2b-d), which may give the evidence of intermediate state of graphene flakes cutting into monodisperse Gdots.

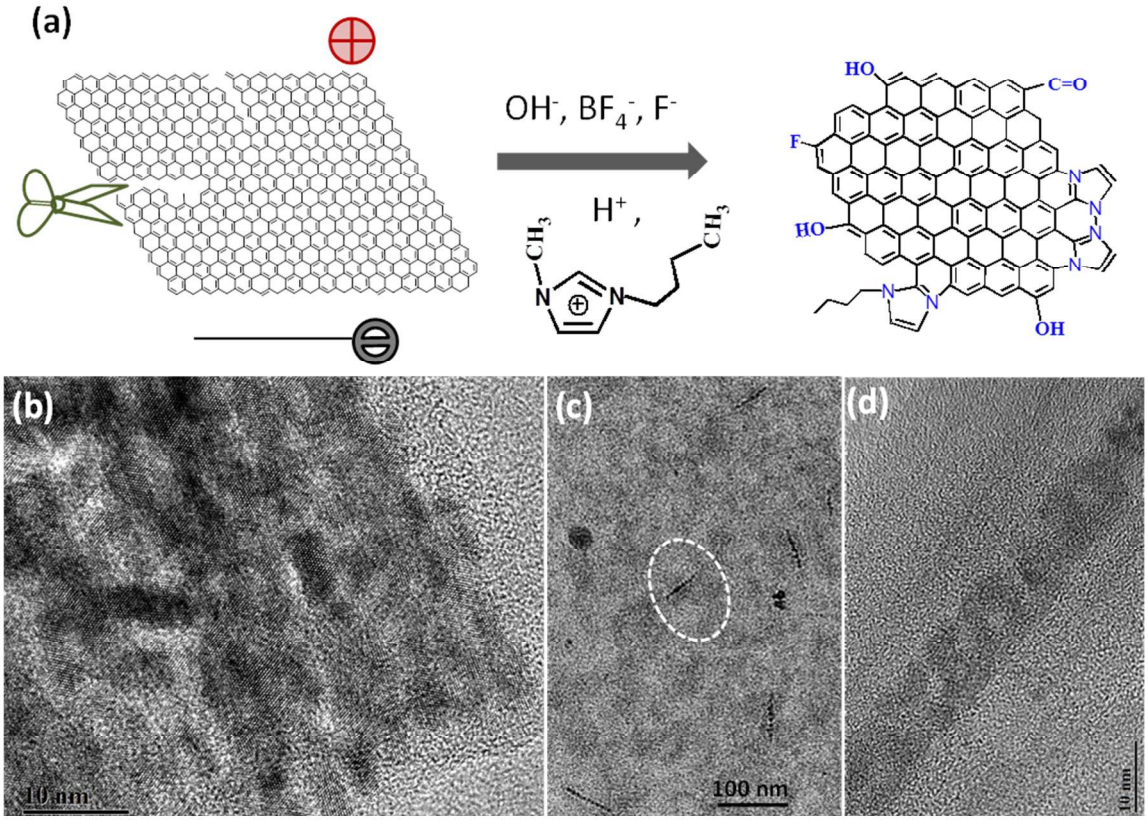

Fig. 5 (a) Schematic illustration of graphene flakes etched by electrochemical redox reaction in ion liquid/water electrolyte under reverse potential. (b-d) TEM images of the etching of nanosheets (b) and line (c,d) from graphene flakes into dots.

The electrocatalytic activity of the multi-heteroatom doped Gdots for the oxygen reduction reaction (ORR) is of particular interest and thus has been investigated in our studies. As shown in Fig.6b, a well-defined cathodic peak clearly occurred in the O_2-saturated but not N_2-saturated 0.1 mol/L of KOH solution for Gdots. The ORR onset potential was at as low as −0.25 V with a remarkable reduction peak at −0.45 V and there is a 70-time enhancement in voltametric currents in O_2 saturated 0.1 M KOH solution compared to that in the N_2 saturated KOH, which demonstrated that the Gdots exhibit great catalytic ability for

the ORR. Although the current density per mass for Gdots is lower than one for commercial Pt/C of 20wt% Pt supported by carbon black, the current from capacitance for Gdots sample under N_2 atmosphere is much lower than that of Pt/C. This suggested the current density enhancement in O_2 over N_2 condition indeed resulted from electrocatalytic acitivity for ORR. Fig.6c showed linear-sweep voltammetry (LSV) curves of the ORR for Gdots at various electrode rotating rates ranging from 400 to 2025 rpm. The measured current density shows the typical increase with increasing rotation rate due to the enhanced diffusion of electrolytes. The transferred electron number per O_2 molecule involved in the ORR process is determined using the Koutecky−Levich equation; and the corresponding curves are plotted for different potentials (Fig.6d). The parallel and straight fitting lines imply a first-order reaction with respect to dissolved oxygen. The *n* value for Gdots is calculated to be 2.0 over the potential range from −0.40 to −0.50 V, suggesting a two-electron process for the ORR on the Gdots electrodes.[43,44]

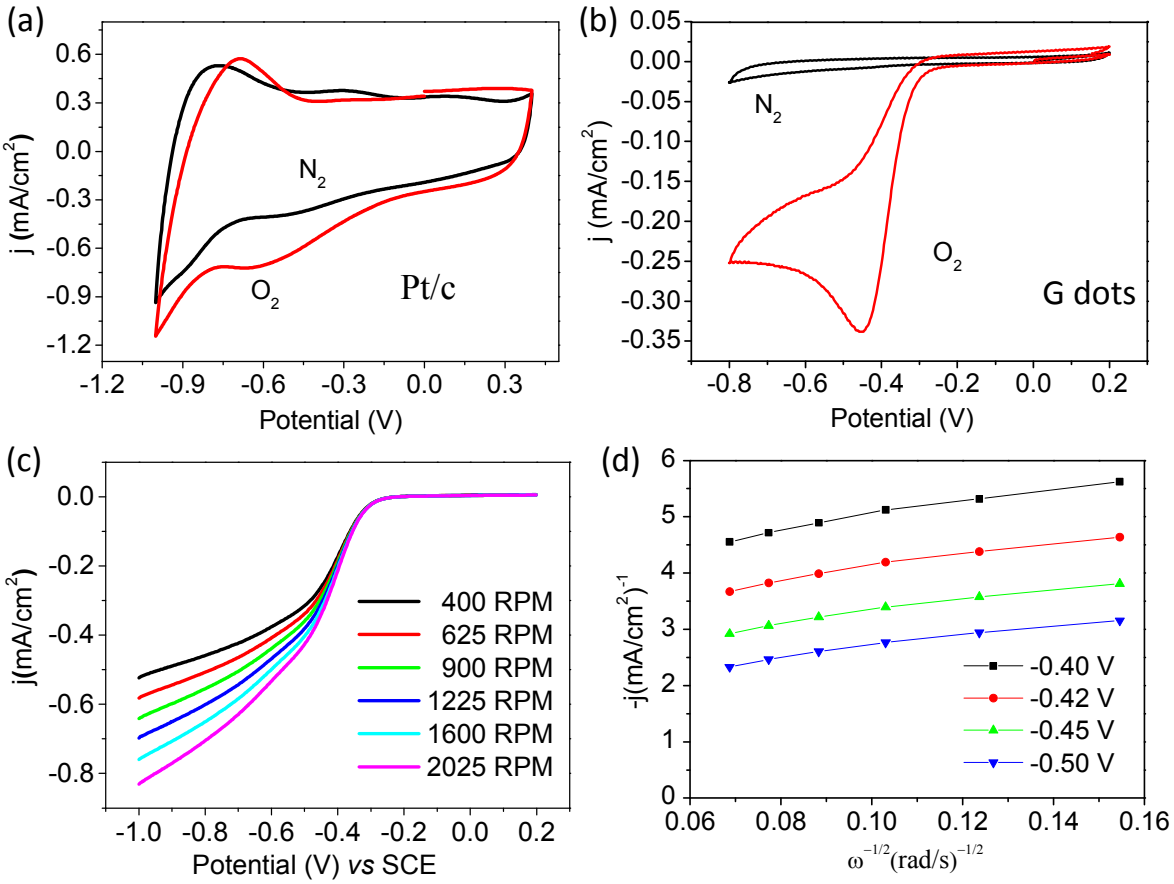

Fig. 6 (a) CVs of Gdots on a glassy carbon (GC) electrode in N_2-saturated 0.1 M KOH, O_2-saturated 0.1 M KOH, (b) Rotating disk electrode (RDE) curves for Gdots in O_2-saturated 0.1 M KOH with various scanning rates. (c) Voltamperograms for oxygenreduction on a glassy carbon electrode in O_2-saturated 0.1 M KOH at various rotation speeds; scan rates, 10 mV s-1. (d) Koutecky-Levich plot of Gdots without thermal treatment at -4.0 V - -0.5V.

We noted that the ORR performance in basic environment of 0.1 mol/L of KOH is some better than acid condition of 0.1 mol/L of $HClO_4$. This may be helpful for review the mechanism of ORR. The electron rich elements of O^- atom in basic condition (rather than –OH in acidic condition) and pyrrolic N as well as F atom could donate graphene electron cloud while charged quaternary N atoms backdonated electrons from adjacent C-C orbitals. The uneven charge distribution from electron donation and backdonation induced by heteroatoms processes facilitate O_2 dissociation and reduction at negative potential.[6-10]

It is interesting and important to investigate the cytotoxicity and cellular imaging of the resulting Gdots. In-vitro cytotoxicity and fluorescent labeling of these Gdots to certain animal tumor Vero cells and normal NRK cells were along investigated. Fig.7 shows the viability of Vero cells and incubated NRK cells with G dots versus the concentrations of Gdots for several days. It was observed that Gdots have slight

lower cell viability than the control group without Gdots adding. The viability values of cells cultured with Gdots have a negative correlation with the Gdots concentration from 5 to 50 μg/ml, which indicates that Gdots have abit inhibiting effects on cell proliferation. However, there is no serious toxicity to cells for the Gdots at the concentration up to 50 μg/ml. Fig.8 shows fluorescence labeling of Vero cells and NRK cells using the Gdots. Our observation demonstrated the Gdots could be potentially applied for bioimaging and drug delivery.[44]

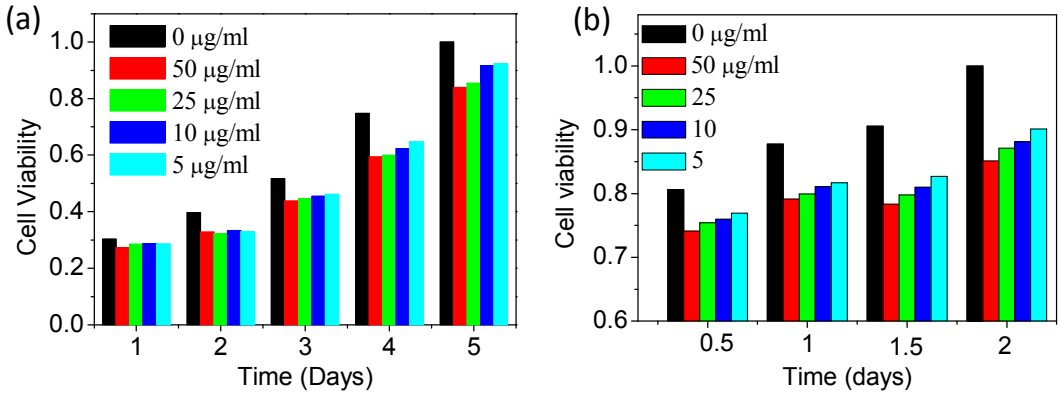

Fig. 7 In vitro cytotoxicity of Gdots to cells. (a) Vero cells for the time from 1 day to 5 day, (b) Normal Rat Kidney Epithelial Cells (NRK Line) for the time from 0.5 day (12h) to 2 day (48h).

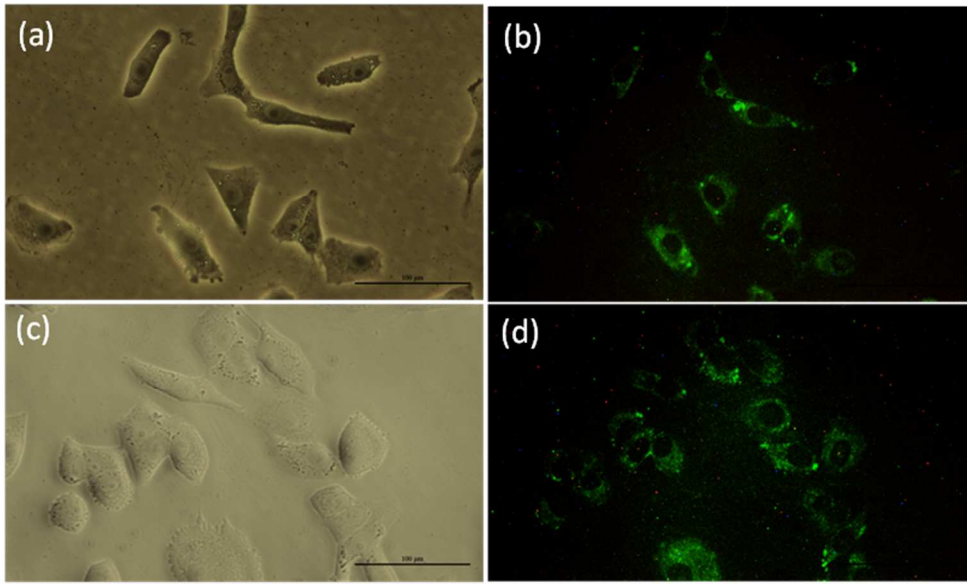

Fig. 8 Bioimaging photographs of optical (a,c) and fluorescent (b,d) of (a,b) Vero cells and (c,d) NRK cells. (Excitation wavelength is 450 nm, Scale bar 100 μm).

4. Conclusions

We have developed a green electrochemical method of cutting high-quality few-layer of graphene flakes into high quality of graphene quantum dots (Gdots). The Gdots clearly exhibit the structure features of high crystallinity and zigzag edges and multi-heteroatom doping as well as 3-8 nm narrow size distribution. The doping of the Gdots by multi-elements of O- and N- and F- elements or rich functional groups were realized in the potential/current exchangeable electrochemical etching process without any thermal treatment. Good electrocatalytic performance of 70-time enhancement of the current density in O_2 over N_2 for oxygen reduction reaction (ORR) was obtained when Gdots were used as the metal-free electrocatalysts in KOH solution. The rich edges and heteroatom-doping of Gdots may facilitate the formation of catalytic sites for ORR. It was found that the Gdots in water exhibit very low in-vitro cytotoxicity to Vero cells and NRK cells. The green

electrochemical approach of high quality of Gdots may direct us in future endeavors towards the rational design and synthesis of graphene-based nanocatalysts for the ORR and biological activity.

Acknowledgements

The authors gratefully acknowledge the support for this work from the National Natural Science Foundation of China (Grant 21373255) and the Hundred Talent Program of the Chinese Academy of Sciences (Grant 2013SCXQT01). We thank Professor Chunxiang Lu and Professor Zhenping Zhu in Institute of Coal Chemistry to allow using Raman and photoluminescence instruments, respectively.

Notes

[a] Key Laboratory of Carbon Materials, Institute of Coal Chemistry, Chinese Academy of Science,Taiyuan,030001, P R China.
[b] University of Chinese Academy of Sciences, Beijing 100049, P R China.
[c] College of Life sciences and Bioengineering, Beijing Jiaotong University, Beijing 100044, P R China.
*Corresponding authors. Tel: 86-351-4040407. E-mail: wangjz@sxicc.ac.cn (J.Z. Wang). Tel: 86-10-51688577. E-mail: dkjian@bjtu.edu.cn (K.J. Ding).

References

1 B. Winther-Jensen, O. Winther-Jensen, M. Forsyth and D. R. MacFarlane, *Science*, 2008, **321**, 671.
2 V. Neburchilov, H. Wang, J. J. Martin and W. Qu, *J Power Sources*, 2010, **195**, 1271.
3 S. Guo, S. Zhang and S. Sun, *Angew. Chem., Int. Ed.*, 2013, **52**, 8526.
4 G. Wu, K. L. More, C. M. Johnston and P. Zelenay, *Science*, 2011, **332**, 443.
5 M. K. Debe, *Nature*, 2012, **486**, 43.
6 L. Zhao, R. He, K. T. Rim, T. Schiros, K. S. Kim, H. Zhou, C. Gutiérrez, S. P. Chockalingam, C. J. Arguello, L. Pálová, D. Nordlund, M. S. Hybertsen, D. R. Reichman, T. F. Heinz, P. Kim, A. Pinczuk, G. W. Flynn and A. N. Pasupathy, *Science*, 2011, **333**, 999.
7 S. Guo, S. Sun, *J. Am. Chem. Soc.* 2012, **134**, 2492.
8 L. Qu, Y. Liu, J.-B. Baek and L. Dai, *Acs Nano*, 2010, **4**, 1321-1326.
9 Q. Xue, H. Huang, L. Wang, Z. Chen, M. Wu, Z. Li, D. Pan, *Nanoscale*, 2013, 5, 12098.
10 Y. Li, Y. Zhao, H. Cheng, Y. Hu, G.Q. Shi, L.M. Dai, L.T. Qu. J Am Chem Soc. 2012, **134**, 15.
11 K. Gong, F. Du, Z. Xia, M. Durstock and L. Dai, *Science*, 2009, **323**, 760.
12 S. Wang□, E. Iyyamperumal□, A. Roy, Y. Xue, D. Yu and L. Dai, *Angew. Chem., Int. Ed.*, 2011, **50**, 11756.
13 W. Yang, T.-P. Fellinger and M. Antonietti, *J. Am. Chem. Soc.*, 2010, **133**, 206.
14 Y. Zheng, Y. Jiao, J. Chen, J. Liu, J. Liang, A. Du, W. Zhang, Z. Zhu, S. C. Smith, M. Jaroniec, G. Q. Lu and S. Z. Qiao, *J. Am. Chem. Soc.*, 2011, **133**, 20116.
15 Z.-H. Sheng, L. Shao, J.-J. Chen, W.-J. Bao, F.-B. Wang and X.-H. Xia, *Acs Nano*, 2011, **5**, 4350.
16 L. Lai, J. R. Potts, D. Zhan, L. Wang, C. K. Poh, C. Tang, H. Gong, Z. Shen, J. Lin and R. S. Ruoff, *Energy Environ. Sci.*, 2012, **5**, 7936.
17 Y. Tan, C. Xu, G. Chen, X. Fang, N. Zheng and Q. Xie, *Adv. Funct. Mater.*, 2012, **22**, 4584.
18 C. Cheng and D. Li, *Adv. Mater.*, 2013, **25**, 13.
19 X. Zhang, J. Yu, C. Wu, Y. Jin, Y. Rong, F. Ye and D. T. Chiu, *Acs Nano*, 2012, **6**, 5429.
20 G. Eda and M. Chhowalla, *Adv. Mater.*, 2010, **22**, 2392.
21 L. Li, G. Wu, G. Yang, J. Peng, J. Zhao and J. J. Zhu, *Nanoscale*, 2013, **5**, 4015.
22 J. Lu, P. S. E. Yeo, C. K. Gan, P. Wu and K. P. Loh, Nature Nanotech. 2011, 6, 247.
23 R. Liu, D. Wu, X. Feng and K. Müllen, *J. Am. Chem.Soc.*, 2011, **133**, 15221.
24 S. Zhu, Q. Meng, L. Wang, J. Zhang, Y. Song, H. Jin, K. Zhang, H. Sun, H. Wang and B. Yang, *Angew. Chem., Int. Ed.*, 2013, **52**, 3953.
25 J. Peng, W. Gao, B. K. Gupta, Z. Liu, R. Romero-Aburto, L. Ge, L. Song, L. B. Alemany, X. Zhan, G. Gao, S. A. Vithayathil, B. A. Kaipparettu, A. A. Marti, T. Hayashi, J.-J. Zhu and P. M. Ajayan, *Nano Lett.*, 2012, **12**, 844.
26 Y. Dong, H. Pang, H. B. Yang, C. Guo, J. Shao, Y. Chi, C. M. Li and T. Yu, Angew. Chem., Int. Ed., 2013, 52, 7800.
27 C. Hu, Y. Liu, Y. Yang, J. Cui, Z. Huang, Y. Wang, L. Yang, H. Wang, Y. Xiao and J. Rong, *J. Mater. Chem. B*, 2013, **1**, 39.
28 L.-L. Li, J. Ji, R. Fei, C.-Z. Wang, Q. Lu, J.-R. Zhang, L.-P. Jiang and J.-J. Zhu, Adv. Funct. Mater., 2012, 22, 2971.
29 L. Zheng, Y. Chi, Y. Dong, J. Lin and B. Wang, J. Am. Chem. Soc., 2009, 131, 4564.
30 Q. L. Zhao, Z. L. Zhang, B. H. Huang, J. Peng, M. Zhang and D. W. Pang, Chem. Commun., 2008, 5116.
31 J. Lu, J.-X. Yang, J. Wang, A. Lim, S. Wang and K. P. Loh, Acs Nano, 2009, 3, 2367.
32 J. Wang, K. K. Manga, Q. Bao and K. P. Loh, J. Am. Chem. Soc., 2011, 133, 8888.
33 Z. Wang, R. Jia, J. Zheng, J. Zhao, L. Li, J. Song and Z. Zhu, Acs Nano, 2011, 5, 1677.
34 Z. Zhang, J Zhang, N. Chen and L. Qu, Energy Environ. Sci., 2012, 5, 8869.
35 Q. Li, S. Zhang, L. Dai and L.-S. Li, J. Am. Chem.Soc., 2012, 134, 18932.
36 M. Ammam and E. B. Easton, Electrochim Acta, 2011, 56, 2847.
37 J. Wang, C.-F. Wang and S. Chen, *Angew. Chem., Int. Ed.*, 2012, **124**, 9431.
38 S. Yasuda, L. Yu, J. Kim and K. Murakoshi, *Chem. Commun.*, 2013, **49**, 9627.
39 N. Liu, F. Luo, H. Wu, Y. Liu, C. Zhang and J. Chen, Adv. Funct. Mater., 2008, 18, 1518.
40 E. J. Biddinger and U. S. Ozkan, J. Phys. Chem. C, 2010, 114, 15306.
41 P. Hapiot and C. Lagrost, *Chem Rev*, 2008, **108**, 2238.
42 Ç. Ö. Girit, J. C. Meyer, R. Erni, M. D. Rossell, C. Kisielowski, L. Yang, C.-H. Park, M. F. Crommie, M. L. Cohen, S. G. Louie and A. Zettl, *Science*, 2009, **323**, 1705.

43 R. Silva, D. Voiry, M. Chhowalla and T. Asefa, *J. Am. Chem. Soc.*, 2013, **135**, 7823.
44 S. Qu, X. Wang, Q. Lu, X. Liu and L. Wang, Angew. Chem., Int. Ed., 2012, 124, 12381.